RIN14B: a pancreatic δ-cell line that maintains functional ATP-dependent K^+ channels and capability to secrete insulin under conditions where it no longer secretes somatostatin

Robert Bränström[a], Anders Höög[b], Martin A. Wahl[1,a], Per-Olof Berggren[a], Olof Larsson[b,*]

[a]*Rolf Luft Center for Diabetes Research, Department of Molecular Medicine, L1:02, Karolinska Institute, Karolinska Hospital, S-171 76 Stockholm, Sweden*
[b]*Department of Pathology, Karolinska Institute, Stockholm, Sweden*

Received 27 May 1997

Abstract The δ-cell line RIN14B was characterized with regard to ATP-regulated K^+ (K_{ATP}) channel activity and hormone release. By applying the patch-clamp technique, dose–response curves for ATP and the sulfonylurea tolbutamide were obtained in inside-out patches. The concentration causing half-maximal K_{ATP} channel inhibition was found to be 23.7 and 27.6 μM for ATP and tolbutamide, respectively. ADP and diazoxide stimulated K_{ATP} channel activity, an effect dependent on the presence of intracellular Mg^{2+}. The stimulatory effect of diazoxide also required the presence of ATP. The kinetic properties of the K_{ATP} channel were analysed in the presence of ATP, a combination of ADP and ATP and in nucleotide-free solutions. The distribution of K_{ATP} channel open time could be described by a single exponential function with a time constant of approximately 30 ms in nucleotide-free and in ATP-containing solutions. The presence of both ATP and ADP resulted in the appearance of an additional time constant of >150 ms. Single-channel unitary current–voltage (*i-V*) relation was characterised for the K_{ATP} channel present in RIN14B cells. The slope conductance, measured at the reversal potential was found to be 19.1 ± 2.4 pS. The permeability for K^+ ions was calculated to be 0.31×10^{-13} $cm^3 \cdot s^{-1}$. We have not been able to confirm the somatostatin releasing profile of the RIN14B cells using radioimmunoassays, nor could we find positive somatostatin stain with immunocytochemical techniques. We conclude that the RIN14B cell line, previously characterized as a somatostatin-secreting cell line, contains K_{ATP} channels with properties closely resembling the K_{ATP} channel described in the pancreatic β-cell. However, the cell line appears to have dedifferentiated with regard to the ability to secrete somatostatin, maintaining the highly differentiated function of both insulin biosynthesis and exocytosis.

Key words: ATP-dependent potassium channel (K_{ATP} channel); Rat insuloma δ-cell line (RIN14B); Somatostatin

1. Introduction

The molecular mechanisms underlying somatostatin release from the pancreatic δ-cell have not been characterized in great detail. Release of somatostatin has been reported to follow release of insulin from the β-cell in the endocrine pancreas, independent of stimuli [1]. Also in patients with non-insulin dependent diabetes mellitus (NIDDM) hormonal abnormalities pertain not only to insulin but also to somatostatin secretion [1]. Thus, there is a decrease in both insulin and somatostatin release in response to glucose. This suggests similarities in the stimulus-secretion coupling between the pancreatic β- and δ-cell. In the β-cell, glucose is metabolized leading to closure of ATP-dependent potassium channels (K_{ATP} channels) due to an increase in the ATP/ADP ratio. The resulting depolarization of the β-cell membrane potential triggers opening of voltage-dependent Ca^{2+} channels, increase in cytoplasmic free Ca^{2+}-concentration, $[Ca^{2+}]_i$, and thereby initiation of insulin secretion. If a similar sequence of events is operating in the secretion of somatostatin, it implies the presence of K_{ATP} channels in the pancreatic δ-cell. The K_{ATP} channel is present in several tissues and was first described in skeletal and cardiac muscle [2–4] and subsequently in insulin-secreting cells [5]. The major problem in obtaining information on the stimulus–secretion coupling in the pancreatic δ-cell, is the relatively low number of these cells in the pancreatic islet. Therefore, an alternative and attractive approach is to use cell lines derived from islet cell tumours. In the present study we have used the established clonal rat pancreatic δ-cell line RIN14B [6,7], originating from the parent RIN-m cell line [8]. In the original characterization of the secretion profile of the RIN14B cell line, it was found that they mainly secrete somatostatin and to some extent insulin [8]. Regarding the identity and characterization of ion channels in the δ-cell, very little is known. Since somatostatin is released from pancreatic islets upon glucose stimulation [1], it is likely that one of the initial steps in the secretory pathway in the δ-cell includes closure of the K_{ATP} channel. In the present study we have made a detailed characterization of the K_{ATP} channel in RIN14B cells, under conditions where we have also investigated cellular contents of somatostatin and insulin and capability of the cells to secrete these two hormones.

2. Materials and methods

2.1. Electrophysiology

2.1.1. Preparation of cells. All experiments were performed using the clonal δ-cell line RIN14B or the clonal β-cell line RINm5F. The RIN14B cell line has previously been described to secrete somatostatin by Gazdar et al. [8]. Cells were grown on Corning Petri dishes (Corning Glass Works, Corning, NY) in RPMI-1640 tissue culture medium containing 11 mM glucose, 10% (w/v) fetal calf serum (Flow Laboratories, Irvine, UK), 2 mM L-glutamine (HyClone, Cramlington, UK), 100 μg/ml streptomycin and 100 IU/ml penicillin (both supplied by Northumbria Biologicals Ltd., Cramlington, UK). The cells were split using Trypsin-EDTA PBS solution (HyClone) and

*Corresponding author. Fax: (46) 8-30-34-58.
E-mail: olof.larsson@molmed.ki.se

[1]*Permanent address:* Department of Pharmacology, Institute of Pharmaceutical Sciences, University Tübingen, Germany.

PII S0014-5793(97)00723-0

kept in culture for 1–3 days at 37°C in an atmosphere of 5% CO_2, prior to experiments.

2.1.2. Solutions. The pipettes were filled with standard extracellular solution containing (in mM): 138 NaCl, 5.6 KCl, 1.2 $MgCl_2$, 2.6 $CaCl_2$ and HEPES–NaOH (pH set to 7.40). The bath solutions (i.e. the 'intracellular' solution) consisted of (in mM): 125 KCl, 1 $MgCl_2$, 10 EGTA, 30 KOH and 5 HEPES–KOH (pH 7.15). Adenosine 5′-triphosphate (ATP) and adenosine 5′-diphosphate (ADP) (both supplied by Sigma Chemical, St. Louis, MO) were added to the 'intracellular' solution, as indicated in text and figure legends. When nucleotides were added as their Na^+ salt, Mg^{2+} was added to maintain an excess of Mg^{2+}. Diazoxide and tolbutamide were prepared as concentrated stock solutions in dimethyl sulfoxide (DMSO), final concentration of DMSO $< 0.1\%$. Patches were excised into nucleotide-free solution and 0.1 mM ATP was first added to test for channel inhibition.

2.1.3. Recordings. All experiments were performed using the inside-out configuration of the patch-clamp technique [9]. This configuration allows free access to the cytoplasmic face of the plasma membrane. Pipettes were pulled from alumino- or borosilicate glass (Hilgenberg, Malsfeld, Germany), coated with Sylgard resin (Dow Corning, Kanagawa, Japan) near the tip and fire-polished. When filled with 'extracellular' solution, the pipettes had a tip resistance of 3–6 MΩ, respectively. Currents were recorded using an Axopatch 200 patch-clamp amplifier (Axon Instruments, Inc., Foster City, CA). During the experiments the current signal was stored on magnetic tape using a video cassette recorder (Super VHS, JVC, Tokyo, Japan) and a modified digital audio processor (VR-10B, Instrutech Corp., Elmont, NY). The recorded signal was stored with an upper cut-off frequency of 2 kHz. With the solutions used, ion currents will be outward (i.e. into the pipette) and channel records are displayed according to the convention with upward deflections denoting outward currents. K_{ATP} channel activity was identified on the basis of the unitary amplitude (1.5–2 pA) and sensitivity to ATP. Before establishment of the seal, the pipette current was adjusted to zero. All experiments were performed at room temperature (20–24°C) and channel activity was measured at 0 mV, if not otherwise indicated.

2.1.4. Data analysis. For analysis of single channel kinetics, records were filtered at 0.2 kHz (−3 dB value) by using an 8-pole Bessel filter (Frequency Devices, Haverhill, MA), digitized at 0.5 kHz using a TL-1 DMA interface (Axon Instruments) and stored in a computer (IBM clone). The degree of channel activity was assessed using in-house software by digitizing segments of the current records (30–70 s long) and forming histograms of baseline and open-level data points. The mean current (i_x) was calculated according to the equation:

$$i_x = \sum_{j=1}^{N} \frac{(I_j - I_B)}{N} \quad (1)$$

where N is the number of samples, I_j is the current observed in sample j and I_B is the value of an user-defined baseline. Analysis of the distribution of K_{ATP} channel open times was restricted to segments of the experiment record containing one to three channel levels using the digitized data. The kinetic constants were derived by approximation of the data to exponential functions by the method of maximum likelihood [10].

Dose-response curves for ATP and tolbutamide were fitted to the Hill equation:

$$i/i_C = \frac{1}{1 + ([X]/K_i)^n} \quad (2)$$

where [X] is the concentration of ATP or tolbutamide, K_i is the concentration of [X] causing half-maximal inhibition and n is the slope parameter corresponding to the Hill coefficient. The i/i_C represents the ratio of mean current found during (i) and prior (i_C) to the experiment. In most inside-out patches channel activity decreased rapidly (run-down) following patch isolation. As shown in Fig. 1, exposing a freshly isolated inside-out patch to ATP, led to an almost complete block of channel activity. Following wash-out of the nucleotide, channel activity increased and reached a maximum activity, which is referred to as the control segment. In the following experiments, test compounds were added ~30 s after the control segment and are referred to as test segment. The mean current test/control ratio for three patches during perfusion with nucleotide-free solutions was calculated to 0.6 ± 0.03 ($n = 3$), and was used to make allowance for the run down of channel activity.

Open probability (P_{open}) was estimated by approximating the observed probability (P_x) of finding x simultaneously active channels, out of a total number of N channels, to the binomial theorem:

$$P_x = \binom{N}{x} P_{open}^x (1 - P_{open})^{(N-x)} \quad (3)$$

Single channel permeability for potassium ions (p_K) can be related to Goldmann-Hodgkin-Katz equation [11]:

$$p_K = i / \frac{VF^2}{RT} \frac{([K^+]_i e^{(VF/RT)} - [K^+]_o)}{(e^{(VF/RT)} - 1)} \quad (4)$$

where V is the reversal potential, and R, T and F denote molar gas constant, temperature in degrees Kelvin (°K) and Faraday's constant, respectively. The $[K^+]_i$ represents the bath solution and the $[K^+]_o$ the pipette solution, containing 5.6 and 155 mM K^+, respectively. Unless otherwise indicated, each experimental condition was tested with identical results in at least five different patches. For figures, records were digitized at 0.16 kHz (if not otherwise indicated) using a DMA interface (Axon instrument). Segments of digitized recordings were exported into CorelDraw (Corel Inc., CA). Values are presented as means ± SD. Channel activity and P_{open} were compared using Student's t-test.

2.2. Cytology, immunocytochemistry and measurements of insulin and somatostatin release

Cells grown in culture for 3 days in Petri dishes were stained with Papanicolaou stain to show cellular morphology. Cells used for immunohistochemistry were grown in Petri dishes, detached, using Trypsin-EDTA, and fixed in 4% formaldehyde in PBS buffer overnight. After centrifugation, the cell block was dehydrated in a graded serie of ethanols followed by xylene and finally embedded in paraffin. Deparaffinized sections were incubated overnight with the following antibodies: somatostatin, monoclonal, 1:600 and 1:200 (Novo Biolabs, Bagsvaerd, Denmark); somatostatin, polyclonal from rabbits, 1:800 and 1:300, (Dakopatt, Glostrup, Denmark); insulin, monoclonal, dilution 1:1000 and 1:300, (Biogenix, San Ramon, CA); insulin, polyclonal from guinea pig, 1:3000 and 1:1000, (a gift from professor Å. Lernmark, Department of Medicine, University of Washington, Seattle, WA). The lower concentration of antibodies served as a positive control, since it is routinely used in our laboratory for sections of pancreatic tissues employing normal formalin fixed paraffin embedded islets. To enhance the sensitivity when studying the RIN14B cell line, we also applied the antibodies at 3 times higher concentrations. For negative controls, the primary antibody was replaced by non-immune sera. The avidin-biotin-complex technique (Vectastain, Vector Laboratories, Burlingame, CA) was used to visualize the antibody–antigen-binding site. Diaminobenzidine was used as chromogen, and Mayer's haematoxylin as counter stain. For hormone measurements, cells were grown in RPMI-1640 medium in 24-well plates. The cells were washed and pre-incubated in a buffer consisting of (mM): 125 NaCl, 5.9 KCl, 1.28 $CaCl_2$, 25 HEPES–NaOH, pH 7.40, and stimulated according to the protocols given in the text. Measurements of insulin and somatostatin release were performed as described previously [12]. Insulin and somatostatin release was analysed radioimmunologically, using rat insulin and somatostatin as standards.

3. Results and discussion

It is evident from a number of studies that glucose and other stimulators of insulin secretion also enhance the release of somatostatin. The parallelism between somatostatin and insulin responses may arise from electrical coupling between δ- and β-cells [13] but can also reflect independent reactions of the two cell types. An explanation for an independent but still virtually identical response pattern for the δ- and β-cells would be that they share a common initial step in their stimulus-secretion coupling. In the β-cell, the K_{ATP} channel serves as a link between glucose metabolism and more distal events

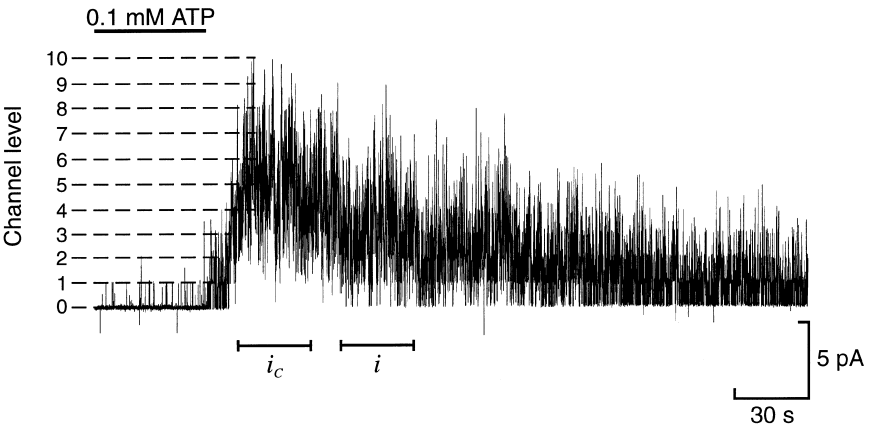

Fig. 1. Time-dependent decline in K_{ATP} channel activity after inclusion of 0.1 mM ATP. The control segment (i_C) is set to ±15 s from maximum channel amplitude and test segment (i) to approximately 60 s after the perfusion of ATP. The mean currents during control and test segment were found to be 7.6 pA and 4.7 pA, respectively.

in the insulin secretory process. In the present study we attempted to identify and characterize a possible K_{ATP} channel in the RIN14B δ-cell line.

3.1. Effects of adenine nucleotides on K_{ATP} channel activity

It is well known that the open probability of the K_{ATP} channel is reduced by application of ATP to the intracellular

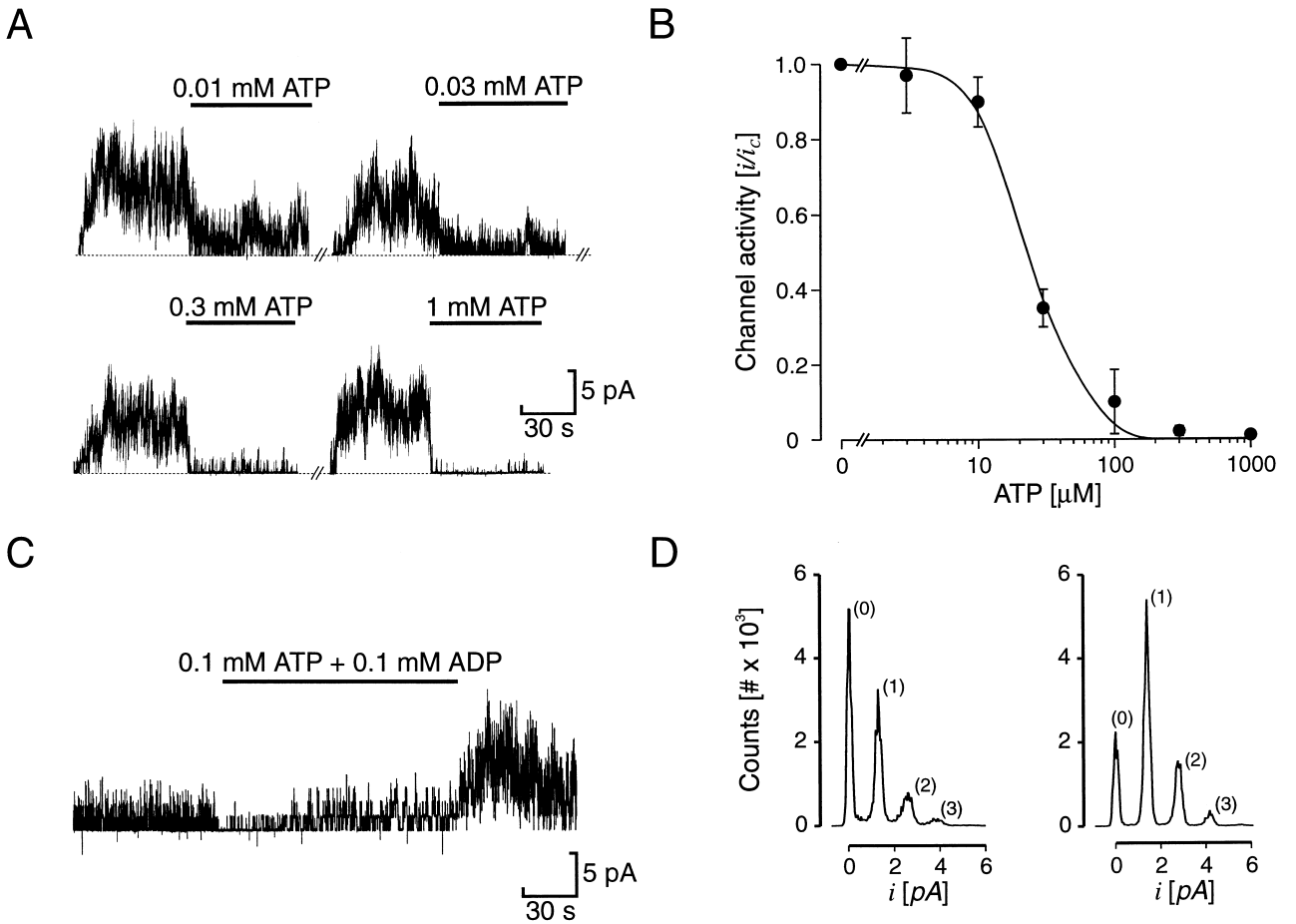

Fig. 2. A: The effect of different ATP concentrations (0.01, 0.03, 0.3 and 1 mM) on K_{ATP} channel activity in an inside-out patch. In between each concentration trial, 0.1 mM ATP was applied. Concentration–inhibition relationship for the inhibition of ATP on the K_{ATP} channel. B: Ordinate shows the ratio of i/i_C. The points show means and vertical bar ±SD (when larger than symbols) ($n = 3$–5). Abscissa shows ATP concentration in μM (logarithmic scale). The line was fitted to Eq. 2 yielding a K_i of 23.7 μM and a slope parameter, n, of 2.21. C: The effect of ADP on the K_{ATP} channel activity and its ability to reactivate the K_{ATP} channel. A mean current in nucleotide-free solution of 1.72 pA was observed which was increased to 2.5 pA in the presence of 0.1 mM ATP and 0.1 mM ADP. A reactivation of the K_{ATP} channel is observed after application of ADP. D: Channel amplitude-histogram in the presence of control-solution (left) and 0.1 mM ADP (right). Ordinate shows integrated time in seconds and abscissa shows current in pA.

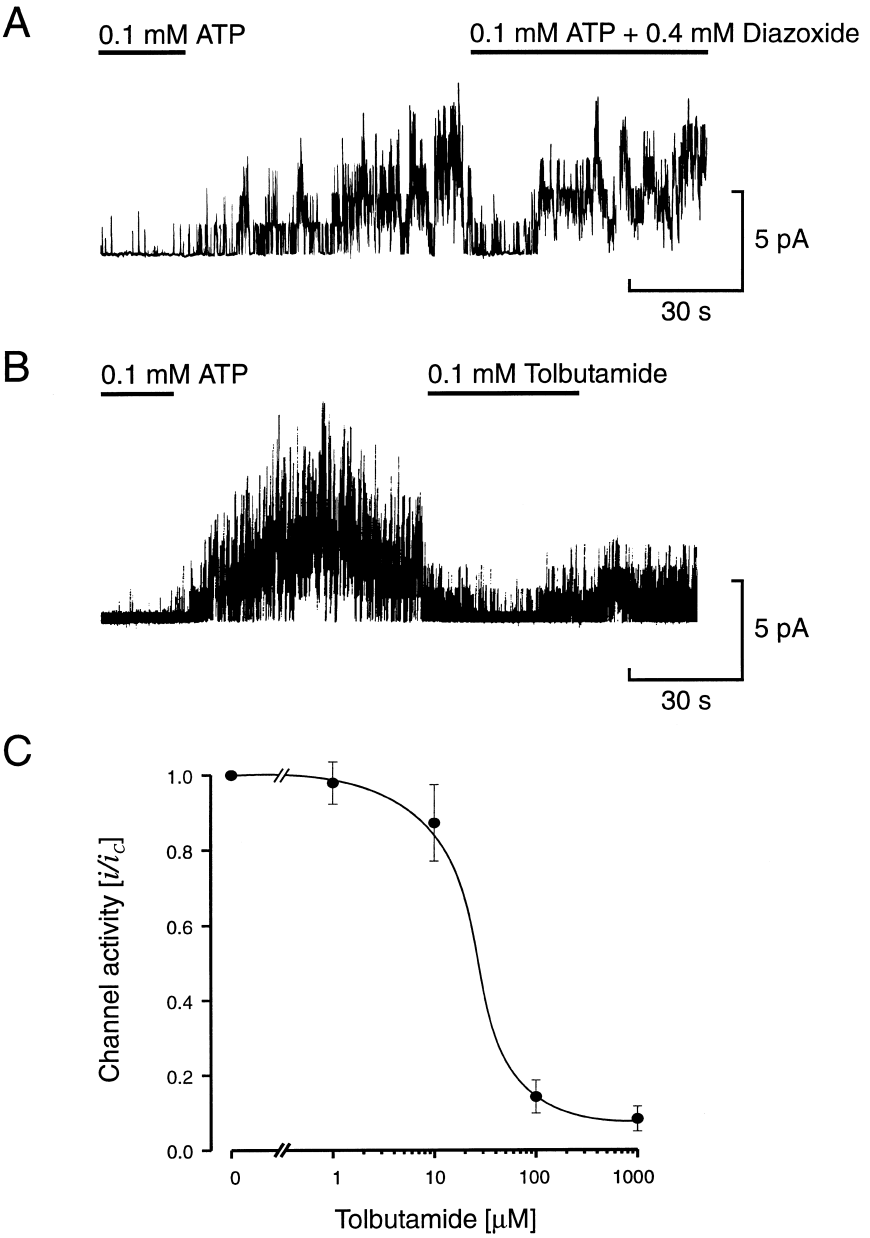

Fig. 3. Record (A) shows the ability of diazoxide to stimulate K_{ATP} channel activity. Mean current prior to diazoxide was estimated to 3.1 pA, which subsequently increased to 3.6 pA during exposure to diazoxide. B: An example trace of the ability of tolbutamide to block the K_{ATP} channel activity in an inside-out patch shortly after patch isolation (<30 s). C: Concentration–inhibition relationship for the action of tolbutamide in closing the K_{ATP} channel. Ordinate shows the ratio of i/i_C. The points show means and vertical bar $\pm$SD ($n=3$–5). Abscissa shows tolbutamide concentration in μM (logarithmic scale). The curve was fitted by hand.

surface of the cell membrane. The characterization of the RIN14B K_{ATP} channel therefore started by assessing the effects of ATP on channel activity, by exposing inside-out patches to a series of concentrations of ATP, interrupted by exposure to nucleotide-free solution. As expected, K_{ATP} channel activity was inhibited with increasing concentrations of ATP. Fig. 2A shows a typical trace of the blocking effect of ATP in excised patches from RIN14B cells. All patches were tested with six different ATP concentrations ranging from 3 to 1000 μM. Channel activity was expressed as the ratio of activity obtained in the presence of the different ATP concentrations and activity estimated in nucleotide-free solution, prior to exposure to ATP. All determinations of channel activity were corrected for channel run-down, as described in the method section. To ascertain a standardized channel reactivation, especially when exposing the patches to low ATP (<0.1 mM ATP) concentrations, the protocol was interrupted by short exposures of the patch to 0.1 mM ATP. In Fig. 2B, compiled data from the concentration–inhibition relation is shown. The mean value points were fitted to Eq. 2, on the assumption that a single molecule of ATP binds to each K_{ATP} channel and close it. The inhibition constant, K_i, was estimated to be 23.7 μM and a Hill coefficient, n, of 2.21 was obtained. Earlier reports have estimated half-maximal inhibition of β-cell K_{ATP} channel activity to 10–50 μM, whereas millimolar concentrations cause a complete block of activity [5,14]. Thus, the sensitivity to ATP of the RIN14B K_{ATP} channel shows a close resem-

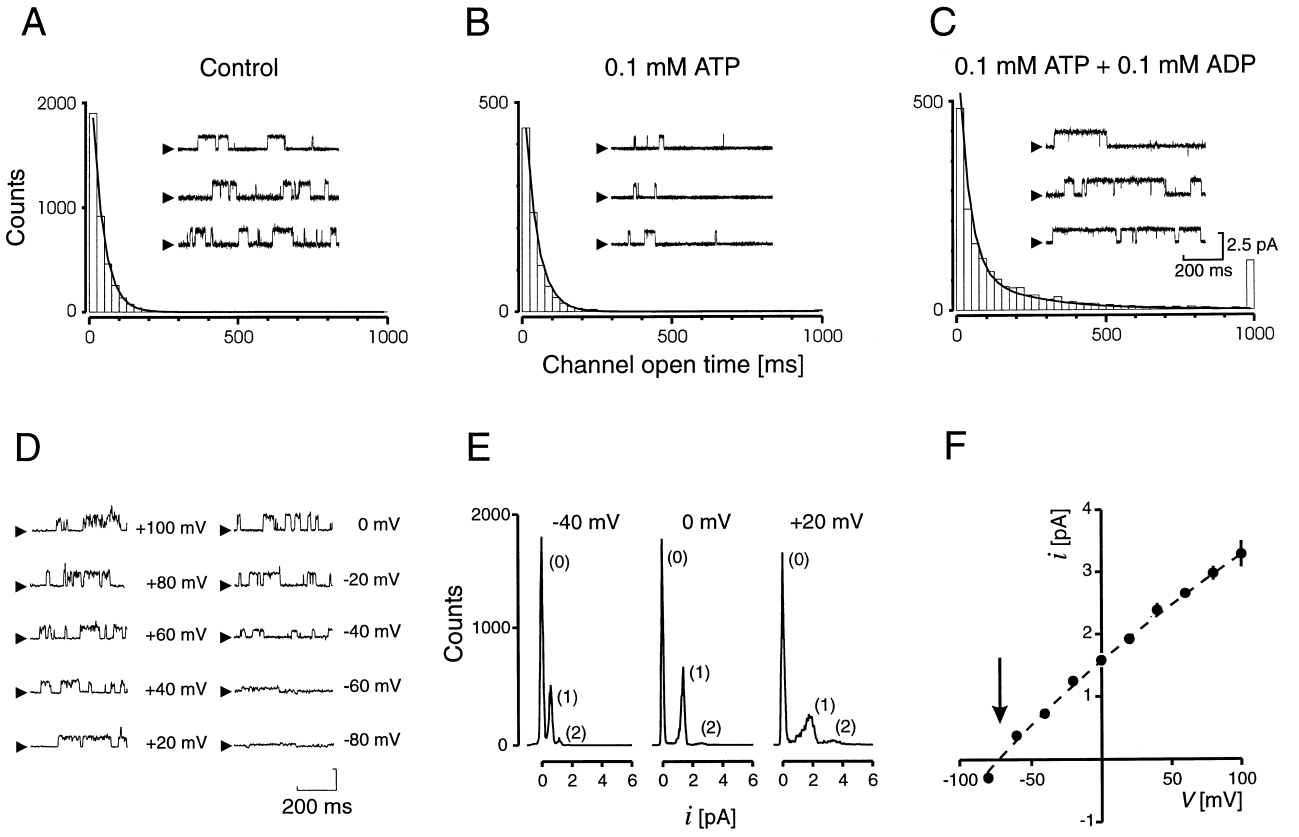

Fig. 4. Distribution of K_{ATP} channel open-time displayed as open-time histograms (A–C). The distribution of channel lifetime could be described by a single exponential function with a time constant $\tau = 35.1$ ms in ATP-free solution (A). A total number of 3850 events were analysed. B: Open-time histogram in the presence of 0.1 mM ATP. A total number of 942 events were analysed and could be fitted by a single exponential function with $\tau = 36.9$ ms. C: The distribution of open-time in the simultaneous presence of ATP and ADP (both 0.1 mM). A total number of 2553 events were analysed and could be best described as the sum of two exponentials with $\tau_1 = 36.6$ and $\tau_2 = 212.1$ ms. Of the total number of channel events, 49.6% belonged to the slow component. The insets show sections of K_{ATP} channel activity recorded under the respective experimental conditions. A sample frequency of 1.0 kHz was used and the bin width was set to 25 ms (A–C). Arrow heads indicate current level when the channel is closed. D: Representative recording of single K_{ATP} channel currents from an inside-out patch in nucleotide-free solution. The pipette potential is indicated to the right of each single channel trace. The arrow heads denote the current level when the channel is closed. The vertical amplitude bar is 5 pA in left column and 2.5 pA in right column. E: Shows K_{ATP} channel amplitude-histogram. Ordinate shows integrated time in seconds and the abscissa indicates channel amplitude in pA. The numbers within parentheses indicate number of simultaneously open channels and zero denotes when the channel is closed. F: Single-channel unitary current–voltage (*i-V*) relation. The symbols indicate mean and vertical bar ± SD ($n = 3$). Ordinate shows pipette potential in mV and the abscissa shows current in pA. E_{rev} is indicated by arrow.

blance to what has been previously reported in the β-cell [15].

The control of K_{ATP} channel activity in the β-cell is believed to result not only from binding of ATP, but also from interaction with ADP. It is well known that ADP counteracts the blocking effect of ATP on the K_{ATP} channel [16]. In Fig. 2C, a combination of 0.1 mM ADP and 0.1 mM ATP was applied to an inside-out patch. It is clear that the blocking effect of ATP is potently counteracted by the presence of ADP also in RIN14B cells. In agreement with earlier reports using β-cells [17], the ability of ADP to stimulate channel activity required the presence of Mg^{2+}. The stimulatory effect of Mg-ADP was quantified by mean current analysis in three patches and showed an increase of 180 ± 36%. This magnitude of Mg-ADP-induced increase in K_{ATP} channel activity is very close to that found in studies with the β-cell [18].

3.2. *Effects of tolbutamide and diazoxide on K_{ATP} channel activity*

Sulfonylureas are a class of drugs known to act as potent and direct inhibitors of the K_{ATP} channel. The K_i for tolbutamide on channel activity has been reported to be in the lower μM range [19] in the β-cell. Fig. 3B shows the blocking effect of tolbutamide on RIN14B K_{ATP} channel activity. A similar protocol as described for the ATP experiments was used, where mean currents during exposure to different concentrations of tolbutamide were compared to currents found prior to exposure to tolbutamide. Compiled results are shown in Fig. 3C. Addition of diazoxide caused an enhancement of K_{ATP} channel currents (Fig. 3A). The ability of diazoxide to stimulate K_{ATP} channel activity has been reported to require the presence of ATP [17]. In a series of experiments, we exposed inside-out patches to 0.4 mM diazoxide in the presence of 0.1 mM ATP. This induced a clear cut increase in channel activity (142 ± 22%; $n = 3$).

3.3. *Kinetic properties of the RIN14B K_{ATP} channel*

In Fig. 4A–C, changes in K_{ATP} channel open time are demonstrated in an inside-out patch from a RIN14B cell, following exposure to nucleotide-free solution and to 0.1 mM ATP,

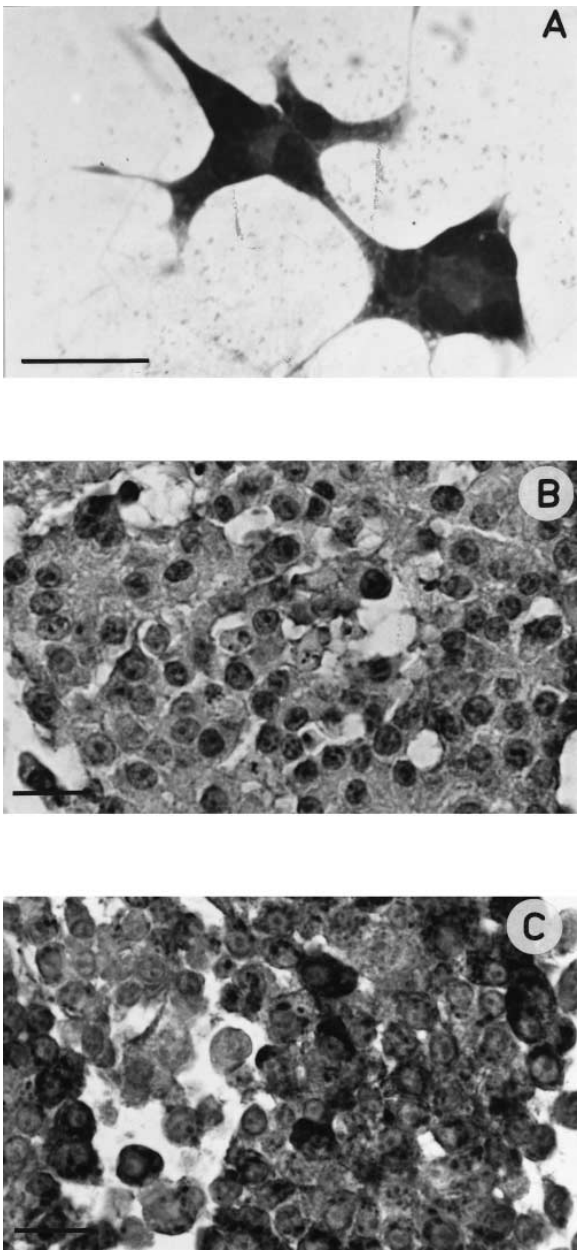

Fig. 5. A: The morphological appearance of RIN14B cells after 3 days of culture displayed apparently well-differentiated cells with elongations reaching nearby cells. No contamination of fibroblasts was seen. Papanicolaou stain, magnification ×640. B: Immunocytochemical staining for somatostatin showed no detectable immunoreactivity in the cytoplasm. The nuclei of the cells were stained dark by haematoxylin. Cells were stained with the avidin-biotin complex method after incubation with high and low concentrations of both monoclonal and polyclonal antibodies. Magnification: ×320. C: Immuno-cytochemical staining for insulin. The techniques used were as in (B). Several cells showed cytoplasmic insulin immunoreactivity (black cells) of various intensity. Bars (A–C): 40 μm.

in the presence or not of 0.1 mM ADP. It is clear that openings observed during exposure to ADP and ATP (Fig. 4C) are much longer than those observed in nucleotide free solution (Fig. 4A) or in the presence of ATP alone (Fig. 4B). We have quantified this effect by analysing the distribution of channel open times in patches not containing more than three simultaneously active channels. In nucleotide free solution, channel activity consisted of relatively short openings. Mean open time was calculated to 40 ± 13 ms ($n = 5$). The distribution of the openings was best fitted by a single exponential. After exposing the patches to ATP alone, channel activity decreased but mean channel open time remained unaffected (43 ± 9 ms; $n = 4$). Also in this case, distribution of openings was best described by a single exponential. In the presence of both ATP and ADP, mean channel open time was dramatically increased to 170 ± 33 ms ($n = 5$) and was best described as a sum of two exponentials.

To further characterize K_{ATP} channel kinetics, we performed a binomial analysis of the amplitude distribution described by Eq. 3. The open probability, P_{open}, for the K_{ATP} channel in nucleotide-free solution was 0.32 ± 0.19 ($n = 5$). When exposed to 0.1 mM ATP, P_{open} was reduced to 0.12 ± 0.1 ($n = 4$). Simultaneously adding ADP and ATP (both 0.1 mM) to the patch resulted in a P_{open} of 0.62 ± 0.21 ($n = 5$; $P < 0.01$, compared to nucleotide-free solution).

Like the K_{ATP} channel present in the pancreatic β-cell, the RIN14B K_{ATP} channel displayed complex kinetic properties. The distribution of channel open time suggested that there are at least two open states similar to those which have been observed in the β-cell [20].

3.4. Channel permeability properties

In Fig. 4D–F, the single channel current–voltage (*i-V*) relation is shown. At 0 mV we estimated the single channel amplitude to be 1.64 ± 0.02 pA ($n = 7$). A reversal potential (E_{rev}) of −75.6 mV was obtained as determined from the intersection with the ordinate (voltage axis). The slope is a second order regression line with a correlation coefficient, r^2, value of 0.998. Measuring the unitary mean slope conductance (γ_s) at the E_{rev} resulted in 19.1 ± 2.4 pS ($n = 4$). This single channel conductance is comparable with results obtained (20–30 pS) using normal ionic gradients ($[K^+]_o \approx 5$ mM; $[K^+]_i \approx 150$ mM) in inside-out patches from the pancreatic β-cell [20–22]. When these values where fitted to Eq. 4 to assess single-channel permeability (p_K) for K^+ ions, the resulting p_K was found to be 0.31×10^{-13} $cm^3 s^{-1}$. This value of p_K may be compared to a p_K value of 0.98×10^{-13} $cm^3 s^{-1}$, reported by Ashcroft et al. [23] for the K_{ATP} channel in the pancreatic β-cell. This discrepancy can be fully explained by the fact that solutions with different ion concentrations were used.

3.5. Secretory properties of the RIN14B cell line

Earlier reports have shown that the origin of the RIN14B cell line is a pancreatic δ-cell [6,7] and that it mainly secretes somatostatin. However, because of the known problem of cell line stability, we reinvestigated the secretory profile of the RIN14B cell line. RIN14B cells were stimulated for 30 min with 25 mM K^+ or with 500 μM tolbutamide. Following analysis of hormone release, we were not able to detect release of somatostatin whereas insulin levels increased 2-fold ($208 \pm 102\%$; $n = 8$). Simultaneous measurements in the RINm5F β-cell line revealed a 4-fold increase in insulin secretion ($392 \pm 157\%$; $n = 8$). Microscopical examination of the cultured RIN14B cells demonstrated a homogenous growth of apparently well-differentiated cells with thin cell extensions (Fig. 5A), which correspond well to the original description of the cell line [8] and indeed to normal δ-cells. There were no signs of fibroblastoid contamination. Immunocytochemical investigation showed no positive somatostatin immunoreactivity (IR) with monoclonal antibodies in high or low concentra-

tions as well as with polyclonal antibodies in low concentration. High concentration of the latter antibody gave a uniform diffuse non-specific reaction. Monoclonal insulin antibodies in high concentration gave positive IR with varied intensity, whereas low concentration gave negative results. Polyclonal antibodies to insulin gave positive IR using both dilutions, with a mixture from intensive IR to nearly negative cells. Hence, the RIN14B cells that we have used secrete insulin but not somatostatin. However, secretion of insulin is less than that of the β-cell line RINm5F, which may reflect the fact that the RIN14B cells are derived from a parent δ-cell.

3.6. Conclusion

The fact that the release of somatostatin follows the release of insulin in the endocrine pancreas, indicates a close resemblance in the stimulus–secretion coupling between the pancreatic β- and δ-cell. This may also suggest that the K_{ATP} channel is involved in the process leading to release of somatostatin in the δ-cell. Our detailed characterization of the K_{ATP} channel in the RIN14B cell, indicated a close resemblance to the K_{ATP} channel described in the pancreatic β-cell. Thus, the K_{ATP} channel in RIN14B cells was inhibited by ATP within an identical ATP-concentration range to that reported in the β-cell. Single channel kinetics, in the presence of various adenine nucleotides, also showed a striking similarity to what we have reported for the β-cell [17]. The sulfonylurea tolbutamide and the sulfonamide diazoxide affected the channel in a way similar to what has been described for the β-cell. Single channel conductance as well as permeability properties were virtually identical to those shown in the pancreatic β-cell.

Our data on secretion indicate that RIN14B cells have dedifferentiated with regard to their secretory properties and were now mainly secreting insulin. In view of the present results, we postulate that the δ-cell line RIN14B undergoes dedifferentiation and loses its capability to secrete somatostatin under conditions where it maintains K_{ATP} channels and ability to synthesize and secrete insulin. In this context, it is of interest to note that after treatment of adult mice with streptozotocin, a population of cells containing somatostatin (SOM^+) and homeodomain-containing transcription factor pancreas duodenum homeobox gene-1 (*PDX-1*$^+$) appeared in pancreatic islets [24]. The appearance of SOM^+/PDX-1^+ cells was followed by the sequential differentiation to SOM^+/insulin-containing cells and to β-cells expressing only insulin.

Acknowledgements: This work was supported by grants from the Swedish Medical Research council (MFR) (04X-09891, 03X-09890, 19X-00034 and 12X-00102), the Swedish Diabetes Association, the Nordic Insulin Foundation, Funds of the Karolinska Institute and Novo Nordisk Pharma AB.

References

[1] S. Efendic, M. Gutniak, and V. Grill, in: V. Grill and S. Efendic (Eds.), The Pathogenes of Non-Insulin-Dependent Diabetes Mellitus, Raven Press, New York, 1988, pp. 271–285.
[2] Noma, A. (1983) Nature 305, 147–148.
[3] Kakei, M. and Noma, A. (1984) J. Physiol. 352, 265–284.
[4] Trube, G. and Hescheler, J. (1984) Pflügers Arch. 401, 178–184.
[5] Cook, D.L. and Hales, C.N. (1984) Nature 311, 271–273.
[6] Bhathena, S.J., Oie, H.K., Gazdar, A.F., Voyles, N.R., Wilkins, S.D. and Recant, L. (1982) Diabetes 31, 521–531.
[7] Amiranoff, B., Lorinet, A.M. and Laburthe, M. (1991) Eur. J. Biochem. 195, 459–463.
[8] Gazdar, A.F., Chick, W.L., Oie, H.K., Sims, H.L., King, D.L., Weir, G.C. and Lauris, V. (1980) Proc. Natl. Acad. Sci. USA 77, 3519–3523.
[9] Hamill, O.P., Marty, A., Neher, E., Sakmann, B. and Sigworth, F.J. (1981) Pflügers Arch. 391, 85–100.
[10] D. Colquhoun, and F.J. Sigworth, in: B. Sakmann and E. Neher (Eds.), Single-Channel Recording, Plenum Press, New York, 1983, pp. 191–263.
[11] Hodgkin, A.L. and Katz, B. (1941) J. Physiol. 108, 37–77.
[12] Corkey, B.E., Glennon, M.C., Chen, K.S., Deeney, J.T., Matschinsky, F.M. and Prentki, M. (1989) J. Biol. Chem. 264, 21608–21612.
[13] Michaels, R.L. and Sheridan, J.D. (1981) Science 214, 801–803.
[14] Ashcroft, F.M. and Kakei, M. (1989) J. Physiol. 416, 349–367.
[15] Ashcroft, S.J. and Ashcroft, F.M. (1990) Cell. Signal. 2, 197–214.
[16] Kakei, M., Kelly, R.P., Ashcroft, S.J. and Ashcroft, F.M. (1986) FEBS Lett. 208, 63–66.
[17] Larsson, O., Ämmälä, C., Bokvist, K., Fredholm, B. and Rorsman, P. (1993) J. Physiol. 463, 349–365.
[18] Hopkins, W.F., Fatherazi, S., Peter-Riesch, B., Corkey, B.E. and Cook, D.L. (1992) J. Membr. Biol. 129, 287–295.
[19] Zünkler, B.J., Lenzen, S., Manner, K., Panten, U. and Trube, G. (1988) Naunyn-Schmiedebergs Arch. Pharmacol. 337, 225–230.
[20] Bokvist, K., Rorsman, P. and Smith, P.A. (1990) J. Physiol. 423, 327–342.
[21] Ashcroft, F.M., Kakei, M. and Kelly, R.P. (1989) J. Physiol. 408, 413–429.
[22] Findlay, I. (1987) J. Physiol. 391, 611–629.
[23] Ashcroft, F.M., Ashcroft, S.J. and Harrison, D.E. (1988) J. Physiol. 400, 501–527.
[24] Fernandes, A., King, L.C., Guz, Y., Stein, R., Wright, C.V.E. and Teitelman, G. (1997) Endocrinology 138, 1750–1762.